Supplementary Information

Differential ligand-selective control of opposing enzymatic activities within a bifunctional c-di-GMP enzyme

Dayna C. Patterson,[1] Myrrh Perez Ruiz,[2] Hyerin Yoon,[3] Johnnie A. Walker,[3] Jean-Paul Armache,[2,4] Neela H. Yennawar,[4*] and Emily E. Weinert [1,2,4*]

[1]Department of Chemistry, The Pennsylvania State University, University Park, PA 16802, USA
[2]Department of Biochemistry and Molecular Biology, The Pennsylvania State University, University Park, PA 16802, USA
[3] Department of Chemistry, Emory University, Atlanta, GA 30322, USA
[4]The Huck Institutes of the Life Sciences, The Pennsylvania State University, University Park, PA 16802, USA

Supplementary Experimental Section

DcpG optimized gene sequence.

ATGCACCACCACCACCACCACATTGAAGGCCGTATGAGCATGATTGAACTGAGCGA
GAAGGACCTGGAGATCGTGCGTAGCATCCGCCCGCTGGTGCTGGAGCACATTGACG
AAATCGTTGATAGCTTCTACGACAGCGTGCTGCGTGTTGATATTCTGAAGAAACTGA
TCCTGGAGCACAGCCAGATTGAAAAGCTGCGTAAAACCCTGAAGAAACACCTGATC
GAGATGTTCAGCGGTCGTATTGACCCGGAGTTTATCGAAAAGCGTATGCGTATCGCG
ATTGTGCACGAACGTATTGGTCTGAAAACCCGTTGGTACATGGGCGCGTTCCAGAAC
CTGCAAAACGCGTTTATCCACATGCTGAACCTGCACATGCCGGATAAGGAGCGTATG
CTGACCGTGTGCCTGAGCATTACCAAACTGCTGAACCTGGAACAGCAACTGGTTCTG
GAGGCGTATGAAAAGCGTAGCAACGAGAAAATCCAGCACCAAGCGTTCCACGACG
AACTGACCGGTCTGCCGAACCGTCGTATGCTGCAGAAGCGTCTGCAAGAGCGTATC
GAACCGGGTGCGGAGGCGCAGGGTCGTTTTGCGGTGATGGTTCTGGACATTGATCGT
TTTAAGATGATCAACGATAGCCTGGGTCACGCGTATGGCGACCAGTTTCTGAAAATG
GTGAGCAGCCGTCTGCTGGAGGCGGCGGGCGAAGCGAGCAGCTTCATTGCGCGTAT
GGGTGGCGATGAGTTTGCGGTTCTGAGCCCGGCGGATGCGGAACATGACCCGGCGG
ATCTGGCGATGCGTATCATTGAGCAGATCCGTCTGCCGTACCAACTGAACCGTACCG
AATTCTTTGTGACCACCAGCATCGGTATTGCGATCTATCCGGAGCACGGCGTTACCG
CGAGCGAACTGCTGCGTAACGCGGATAAGGCGATGTACGAGGTGAAGAAAGATGGT
AAAAACGACTACCAGTTCTATAGCGCGGCGTTTGATGCGCACCTGCAAGAGAAGAT
TGAGCTGGAAAACGACCTGCGTAAAGCGGTTGCGCGTCAGGAACTGGTGGTTCACT
ACCAGCCGCAATATACCCTGAAGGAGAACCAACTGATCGGTGTGGAAGCGCTGATG
CGTTGGAACCACCCGCGTAAAGGCCTGCTGGATCCGAGCGTTTTCATTCCGATCGCG
GAGGAAACCGGTATGATTTATGAGATGGGTGCGTGGATCCTGCGTGAAGCGTGCCG
TCAGATGCAGGCGTGGCATGATGCGGGTGGCCCGCAGATCCGTGTGAGCGTTAACC
TGAGCACCCAGCAATTTCACCAAAGCAACCTGTGCGAAACCATTCGTGGTATCCTGG
AGGAAACCGGCCTGCCGGCGGAGTACCTGGAGCTGGAAATCACCGAAAGCATGATG
ATGGACGTGACCCGTAGCACCCAGATTCTGCAAGAACTGACCGCGCTGGGTGTTTAT
ATCAGCATGGACGATTTCGGTACCGGCTACAGCAGCCTGAGCTATCTGAAACTGTTC
CCGATTCGTAAGCTGAAAATCGATCGTAGCTTTATGAAGGACGTGATGAGCAACCC
GAACGATAAAGCGATTGTTGCGACCATCATTAGCATGGCGCACCACCTGAACATGC
GTGTGATCGCGGAGGGCGTTGAAACCGAAGACCAGCTGCAATACCTGAGCGAAAAC
GGTTGCGACGATATCCAGGGCTTTTTCTTTAGCCCGCCGGTTACCGCGGAACAACTG
CAAAGCACCATTCTGAGCGGCAAA

Protein expression and purification

The codon-optimized gene for DcpG (accession number EHQ61185; codon optimization performed by GenScript) was cloned into pET-20b(+) using NdeI and XhoI restriction sites. The resulting plasmid was transformed into OverExpress™ C41(DE3) pLysS (Lucigen) via heat shock and positive transformants were selected on LB medium containing ampicillin (DOT Scientific) (100 μg mL^{-1}) and chloramphenicol (Research Products Int.) (30 μg mL^{-1}). An approach known as the plating method was used obtain optimal protein expression.(1) Briefly, a single colony of pet20b(+)-DcpG plasmid containing cells was suspended in 200 mL of autoclaved deionized water and vigorously shaken. The suspension was plated on LB medium containing ampicillin (100 μg

mL^{-1}) and chloramphenicol (30 μg mL^{-1}) and incubated at 37 °C. All colonies were scraped off and suspended in expression media (45 g yeast extract (Research Products Int.), 1.6 g KH_2PO_4 (Research Products Int.), 13.0 g K_2HPO_4 (Research Products Int.), and 1% glycerol (Sigma Aldrich) per 1 L). The cells were grown at 37 °C and aminolevulinic acid (Sigma Aldrich) (500 μM final concentration) was added to the culture at OD_{600} = 0.3. The temperature was lowered to 18 °C and the cells were grown to OD_{600} = 0.7. Cells were then induced with IPTG (Research Products Int.) (0.5 mM) and allowed to express the DcpG protein for 18-20 hours, prior to being harvested by centrifugation (4000 x g. at 4 °C, 20 min) and the resulting cell pellet frozen at -80 °C until use.

For purification, the cell pellet was thawed and suspended in Buffer A (50 mM Tris (Research Products Int.), 300 mM NaCl (Research Products Int.), 20 mM imidazole (Sigma Aldrich), pH 7.5) with protease inhibitors (benzamidine HCl (Research Products Int.), and Pefabloc® SC (Sigma Aldrich). The cells were lysed using a homogenizer (Avestin, Inc.) and the resulting lysate was centrifuged at 130,000 x g in a Beckman Optima L-90X ultracentrifuge at 4 °C for 1 hour. All subsequent purification steps were performed at 4 °C. The supernatant was applied to a pre-equilibrated HisPur Ni-column (Fisher Scientific) and DcpG was eluted with Buffer B (50 mM Tris, 300 mM NaCl, 250 mM imidazole, pH 7.5) at a flow rate of 1.0 mL/min. Purified DcpG was desalted eluting using a S200 gel filtration column (GE Healthcare) that had been equilibrated with Buffer C (50 mM Tris, 50 mM NaCl, 1 mM DTT (Research Product Int.), 5% Glycerol (v/v), pH 7.5) at a flow rate of 1.0 mL/min. Fractions containing DcpG were collected and concentrated via ultrafiltration (YM-10, 10 kDa MWCO filter, Millipore), aliquoted, flash frozen, and stored at -80 °C until use. Protein purity was assessed by sodium dodecyl sulfate-polyacrylamide gel electrophoresis (SDS-PAGE) and concentrations were determined using the Bradford Microassay (Bio-Rad Laboratories). DcpG is present as a dimer but denatures to mostly a monomer on SDS-PAGE gel, with a small residual dimer band.

Electronic spectroscopy

UV-visible spectra were acquired from 800 nm to 200 nm using an Agilent Cary 100 spectrophotometer with Agilent Technologies Cary Temperature Controller. Spectra were recorded in a 1 cm path length quartz cuvette. Preparation of complexes was carried out as previously described except that the proteins were prepared in Buffer C.(2, 3) Briefly, DcpG is purified in the Fe(II)-O_2 ligation state. A 200 μL aliquot of 80 uM DcpG is transferred into the anaerobic chamber where a solution of 500 μM sodium dithionite (Millipore Sigma) is prepared with anaerobic Buffer C. A 10 μL aliquot of 500 uM sodium dithionite is added to DcpG and left to sit for 30 minutes. The mixture was then desalted using a PD-10 column that was equilibrated with Buffer C and checked using the spectrophotometer for the fully reduced Fe(II) ligation state. For the Fe(II)-CO ligation state, a stream of CO was blown over the Fe(II) sample. For the Fe(II)-NO sample, 5 μL of 10 mM DEA-NONOate (Cayman Chemical) dissolved in anaerobic 0.1 M NaOH was added to the protein.

DGC enzyme kinetics

Prior to DGC kinetic assays, DcpG and *Ec*DosP(4) were reduced and various DcpG complexes formed as previously described.(2-4) The ligation/oxidation state of the heme was determined by UV-vis spectroscopy before each enzyme assay. All Fe(II), Fe(II)-NO, and Fe(II)-CO kinetics were measured in an anaerobic chamber (Coy Laboratories). The EnzChek pyrophosphate kit (Life

Technologies) was used according to the manufacturer's instructions with the exception that DcpG and a phosphodiesterase (*Ec*DosP) were added, and the reactions were initiated with varying concentrations of GTP (Sigma), as described for other GCS proteins.(5, 6) Briefly, the EnzChek kit monitors production of pyrophosphate from the enzymatic conversion of GTP to c-di-GMP. The kit contains an inorganic pyrophosphatase (IP) and nucleotide phosphorylase (NP). PPi is converted to Pi via IP and the resulting Pi is used to enzymatically convert 2- amino-6-mercapto-7-methylpurine ribonucleoside (MESG) to ribose 1-phosphate and 2- amino-6-mercapto-7-methylpurine. The enzymatic conversion of MESG results in a shift in absorbance maximum from 330 nm to 360 nm. A360 readings were monitored every 30 seconds for 180 minutes.

Assays were performed in triplicate in 96 well plates containing 4 protein concentrations (0.25-2.5μM) and 5 GTP concentrations (0-1000 μM). *Ec*DosP was included at 3-fold molar excess to eliminate inhibition of cyclase activity by the produced c-di-GMP (**Figure S1**). Plates were monitored using an Epoch2 plate reader and Gen5 software (Biotek). The entire plate assay (including triplicates) was repeated at least twice with different protein preparations to account for day to day and protein batch variability. Subsequent analyses to determine enzymatic rates were performed using Igor Pro (Wavemetrics).

PDE enzyme kinetics

Prior to PDE kinetic assays, the proteins were reduced, and various complexes formed as previously described,(2, 3) and ligation/oxidation state of the heme was determined by UV-vis spectroscopy. All Fe(II), Fe(II)-NO, and Fe(II)-CO kinetics were measured in an anaerobic chamber. The EnzChek phosphate kit (Life Technologies) was used according to the manufacturer's instructions with the exception that DcpG was added and the reactions were initiated with varying concentrations of c-di-GMP. 5'-nucleotidase from *Crotalus atrox* venom (Enzo Life Sciences) also was added to the kit at a concentration of 100 units/mL per well. 5'-nucleotidase catalyzes the hydrolysis of pGpG to GpG and phosphate but does not hydrolyze c-di-GMP (**Figure S2**). A360 readings were monitored every 30 seconds for 180 minutes.

Assays were performed in triplicate in 96 well plates containing 4 protein concentrations (1.25-10 μM) and 5 c-di-GMP (Axxora) concentrations (0-75 μM). The entire plate assay (including triplicates) was repeated at least twice to account for day to day and protein batch variability. Subsequent analyses to determine enzymatic rates were performed using Igor Pro (Wavemetrics).

Coupled DGC-PDE enzyme kinetics

The dual enzyme activity of Fe(II), Fe(III), Fe(II)-O_2 and Fe(II)-NO DcpG DGC-PDE in the absence of heterologous enzymes was determined by HPLC analysis. The enzyme assays were adapted from procedures described previously.(7, 8) The reaction mixture contained final concentration 2.5 μM DcpG in its correct ligation state and 10 mM $MgCl_2$. The Fe(II), Fe(II)-O_2 and Fe(II)-NO reactions contained 50 mM Tris pH 7.5, 50 mM NaCl, 1 mM DTT, 5% glycerol to a final volume of 900 μL. The Fe(III) reactions contained 50 mM Hepes pH 7.5, 50 mM KCl, and 5% glycerol to a final volume of 900 μL. To initiate the reactions, 100 μL of 5 mM GTP (Alfa Aesar) was added to a final concentration of 500 μM. To follow the rate of the nucleotides formation and consumption, 100 μL aliquots were withdrawn at time intervals and the reactions were stopped with 25 μL of 0.5 M EDTA then heated at 90 ºC for 10 min. Then precipitate proteins were removed by centrifugation at 12,000 rpm for 10 min then placed on ice. The supernatants

were then run on an Agilent C18 HPLC reversed phase column, using an Agilent HPLC System. The mobile phase consisted of (A) 0.15 M NaH2PO4, pH 5.2 and (B) 40% acetonitrile (balance A eluent). A linear gradient from 0–35% B for 10 min at 1 ml/min was used to separate c-di-GMP, and pGpG. Known quantities of c-di-GMP and pGpG nucleotides were used for standardization.

Quantification of *P. dendritiformis* biofilm formation by Congo Red staining

Biofilm quantification with performed as previously described.(9) Individual colonies of *P. dendriformis C454* were inoculated into 5 ml sterile LB containing and cultured overnight in 15-ml plastic culture tubes at 30 ºC. The overnight cultures were inoculated 1:35 into 7 ml of LB containing 1% glucose and 0.0025% Congo red in 15 ml VWR centrifuge tubes (sterile, polypropylene). One milliliter of each sample from each bio-replicate was then transferred to a 5-ml culture tube (sterile, polypropylene). This was repeated three times for each bio-replicate. The cultures were incubated for 24 h at 30 ºC with shaking at 100 rpm. For anaerobic growth, the samples were prepared in anaerobic chamber (Coy Labs) using anaerobic LB 1% glucose. The samples were then placed into a sealed glass container containing an Anaerobic Gas Pak and then 24 h at 30 ºC with shaking at 100 rpm. For growth in the presence of nitric oxide, DETA-NONOate (Cayman Chemicals) was added to anaerobic LB containing 1% glucose to a final concentration of 100 µM and left to incubate in anaerobic chamber for 12 h before inoculating with overnight culture. The samples were then placed into a sealed glass container containing an Anaerobic Gas Pak and then 24 h at 30 ºC with shaking at 100 rpm. For biofilm quantification, samples were centrifuged at 12000 rpm for 20 min and 200 µL of supernatant were transferred to a 96-well microplate (Corning Costar; sterile, non-treated, polysterene). The absorbance at 500 nm was recorded using a microplate reader. For normalization, each culture was gently vortexed and 200 µL transferred to a 96-well microplate prior to recording the OD_{600} using a microplate reader.

Biofilm formation of *E. coli* expressing DcpG

Biofilm quantification with performed as previously described.(9) *E. coli* C41 (DE3) cells with pET20b-DcpG plasmid, generated as described in the Protein expression and purification session, were used to assess the effects of gases on DcpG-dependent biofilm formation.

O_2 dissociation rates

O_2 dissociation rates were performed as previously described with the following modifications.(2, 5, 10) DcpG and variants (3-5 µM) for O_2 dissociation rates and a 10mM sodium dithionite trap were prepared in anaerobic Buffer C in anaerobic chamber (Coy Labs). Saturating CO was not used as part of the trap. The dissociation of O_2 from the heme was monitored using an SX20 stopped flow equipped with a diode array detector and fit globally using Pro-KII (Applied Photophysics). Additional fitting analysis of raw data was performed using Igor Pro (Wavemetrics). To confirm that the O_2 dissociation rate was independent of sodium dithionite concentration, multiple sodium dithionite concentrations with and without CO were tested (**Table S2, S3**).

NO dissociation rates

NO dissociation rates were performed similar to O_2 dissociation rates. The dissociation of NO from the heme was monitored at 25 °C following mixing of 10 µM of DcpG Fe(II)-NO in Buffer C with different sodium dithionite concentrations using an SX20 stopped flow equipped with a diode array detector (Applied Photophysics) housed in an anaerobic chamber (Coy Labs). The

concentration of the samples in the different experiments is given as "after mixing"; a 1:1 dilution was always used in the symmetric mixing apparatus. The data was fit globally using Pro-KII (Applied Photophysics) to determine k_1 and k_2. Additional fitting analysis of raw data using the minimum and maximum wavelengths (404 nm and 423 nm) was performed using Igor Pro (Wavemetrics) to determine the percentages of k_1 and k_2. To confirm that the NO dissociation rate was independent of sodium dithionite concentration and CO, multiple sodium dithionite concentrations with and without CO were tested (**Table S2**).

Potentiometric titrations for midpoint potential determination

Electrochemical titrations were performed anaerobically with an optically transparent thin-layer cell (OTTLE). This cell was designed as previously described.(11) Briefly, the OTTLE cell consisted of a 3D printed cuvette spacer (Sculpteo, Inc.) with compartments to hold the reference, working and counter electrodes. The reference was a M-401 Ag/AgCl electrode (Microelectrodes, Inc.) and was calibrated using potassium ferricyanide (+213 mV vs. standard hydrogen electrode). The working electrode consisted of two 0.25 mm thick gold foil plates (Sigma Aldrich) and 0.5 mm thick gold wire. The gold plates were prepared by soaking in 1-propanol (Sigma-Aldrich) solution containing 1% of 1-mercaptohexal (Sigma-Aldrich) to create a monolayer on the electrodes. The counter electrode was a 1 mm thick platinum wire (Sigma-Aldrich). The electrodes were placed in each assigned compartment and then the entire electrode insert was placed in a 10 mM quartz cuvette (Starna Cells). The cell was sealed with a Teflon cap equipped with ports for each electrode.

Mediator mix and sample blank preparation: The mediator stock solution consists of a mixture of seven different mediators at a 1000X stock concentration. Mediators included in the stock solution were duroquinone (Sigma-Aldrich), pyocyanin (Sigma-Aldrich), 2-hydroxy1,4-naphthoquinone (Sigma-Aldrich), anthraquinone-2-sulfonate (Sigma-Aldrich), benzyl viologen (Sigma-Aldrich), phenosafranin (Sigma-Aldrich), indigo carmine(Sigma-Aldrich) and hydrogen hexachloroiridate(IV) hydrate hydrogen hexachloroiridate(IV) hydrate. All mediators were dissolved in degassed DMSO (Sigma-Aldrich) except for benzyl viologen, which was dissolve in anaerobic water. To prepare the 10X mediator mix, 10 µl of each mediator was added to 920 µl of 50 mM Hepes (Reseach Products Int.) 50 mM KCl (Reseach Products Int.) or 100 mM KH_2PO_4 (Reseach Products Int.) 50 mM KCl buffer, depending on titration and pH. To prepare a blank sample for the UV-vis measurement, 45 µl of mediator mix was added to 405 µL of 50 mM Hepes 50 mM KCl buffer or 100 mM potassium phosphate 50 mM KCl buffer, depending on the buffer being used in the titration.

Oxidative titration: To prepare samples for oxidative titration, the OTTLE cell was purged with argon for 20 minutes. A solution containing 405 µL of ~100 µM DcpG Fe(II) and 45 µl of mediator mix was prepared in anaerobic chamber. The buffers used for the oxidative titration were 50 mM Hepes 50 mM KCl or 100 mM potassium phosphate 50 mM KCl. The sample mix was introduced to the to the purged OTTLE cell via a Hamilton syringe. The desired oxidative potentials of the sample were maintained by coulometric generation of mediator-titrant. The potential control by the three-electrode system was achieved by using a CH Instrument Electrochemical Analyzer and the temperature was maintained at 25 ºC using Agilent Technologies Cary Temperature Controller. Additional fitting analysis was performed using Igor Pro (Wavemetrics). Midpoint potentials are quoted relative to the standard hydrogen electrode (SHE).

Reductive titration: To prepare samples for oxidative titration, the OTTLE cell was purged with argon for 20 minutes. DcpG was electrochemically oxidized by the CH Instrument Electrochemical Analyzer. For the chemically oxidized sample, a solution containing 405 µL of ~100 µM DcpG Fe(III) and 45 µl of mediator mix was prepared in anaerobic chamber and the sample mix was introduced to the to the purged OTTLE cell via a Hamilton syringe. For the electrochemically oxidized sample, a solution containing 405 µL of ~100 µM DcpG Fe(II)-O_2 and 45 µl of mediator was held at an oxidizing potential for 14 hrs. The desired reductive potentials of each sample were maintained by coulometric generation of mediator-titrant. The potential control by the three-electrode system was achieved by using a CH Instrument Electrochemical Analyzer and the temperature was maintained at 25 ºC using Agilent Technologies Cary Temperature Controller. Additional fitting analysis was performed using Igor Pro (Wavemetrics; **Equation S1**). Midpoint potentials are quoted relative to the standard hydrogen electrode.

Small-angle X-ray scattering (SAXS)

DcpG WT protein samples at concentrations of 0.25, 0.50, 0.75 and 1.0 mg/mL were prepared in a buffer containing 50 mM Tris 50 mM, NaCl, 5% glycerol pH 7.5. All samples were centrifuged at 14,000 rpm for 20 min to minimize aggregation and to remove dust particles prior to analysis. Synchrotron SAXS data were collected at the macromolecular Cornell High Energy Synchrotron Source, MacCHESS, on the G1 beamline station. Data were collected at 293 K using a dual PILATUS 100K-S SAXS/WAXS detector and a wavelength of 1.264 Å. A 1.5 mm OD quartz glass capillary with 10 µm thick walls *in vacuuo* was used and 30 µl of sample was loaded with a Hudson SOLO single-channel pipetting robot (Hudson Robotics Inc. Springfield, New Jersey). To reduce radiation damage, sample plugs were oscillated in the X-ray beam using a computer-controlled syringe pump. The sample capillary-to-detector distance was 1508.0mm and allowed for simultaneous collection of small- and wide-angle scattering data, covering a broad momentum-transfer range (q range) of 0.0075 – 0.8 $Å^{-1}$ ($q = 4\pi\sin(\theta)/\lambda$, where 2θ is the scattering angle). The energy of the X-ray beam was 9.808 keV, with a flux of 3 X 10^{11} photons/second and a diameter of 250 µm × 250 µm. The synchrotron storage ring was running at 50 milliamps positron current.

Exposure times of 10 seconds in ten 1-second frames were used for the measurements; this allowed monitoring for any radiation damage effect. No radiation damage was detected and the ten frames were averaged. The RAW software was used for initial data reduction and background buffer data subtraction.(12) The data at high concentrations showed no concentration dependence and was used for further analysis. The forward scattering $I(0)$ and the radius of gyration (R_g) were calculated using the Guinier approximation, which assumes that at very small angles ($q < 1.3/R_g$) the intensity is approximated as $I(q) = I(0)\exp[-(qRg)23]$. The molecular mass was estimated using a comparison with glucose isomerase and lysozyme standard protein data and Guinier fit and Kratky plots generated in the BioXTAS RAW software. For all further data analysis, the SAXS software suite ATSAS(13) was used. GNOM(14) was used to calculate the pair-distance distribution function P(r), from which the maximum particle dimension (D_{max}) and Rg were determined (**Table S6**). *Ab initio* low-resolution solution models were reconstructed using DAMMIN(15) for data in the range ($0.009 < q < 0.275$ $Å^{-1}$). Ten models were generated from each program and averaged using DAMAVER(16). The normalized spatial discrepancy parameter (NSD) obtained from DAMAVER indicated the similarity between models used for average

calculations. NSD values ≤ 1.0 were obtained as expected for similar models. The theoretical scattering profiles of the constructed models were calculated and fitted to experimental scattering data using CRYSOL(17) (**Figure S16**).

Individual domains of the DcpG structures, globin, GGDEF and EAL were generated using homology modelling in iTasser(18). Possible tertiary and quaternary structures of globin-globin, EAL-GGDEF, GGDEF-GGDEF, EAL-EAL dimers were also modelled in iTasser and the PyMOL graphics software(19) using the corresponding sub-sequences and available high-resolution protein structures. The linker residues connecting the globin and GGDEF domains were allowed to have random-coil conformations. The various domain models were manually rotated and translated to fit into the SAXS solution envelope using PyMOL. The constraints used for building the DcpG dimer included keeping the established globin dimer intact and using the cross-linking data information for the wild type and mutants for positioning the other domains. The complete DcpG dimer model hence built was energy minimized using the Chimera(20) software. To evaluate the conformational flexibility of the domains in the manually fit dimer, SREFLEX(21) software was used with the domains and their individual dimers refined as independent rigid bodies. This ATSAS program uses normal mode analysis to estimate the flexibility of high-resolution models and improves their agreement with experimental SAXS data. In these refinement steps, the EAL and GGDEF domains were free to adopt different conformations relative to a fixed globin dimer. For conformers that supported a EAL-GGDEF domain association, additional restraints were imposed in SREFLEX to keep it as an intact unit.

Gradient Fixation (GraFix)(22) preparation of the complexes

The purified sample was dialyzed into Buffer A (Buffer A: 20 mM HEPES-KOH pH 7.55, 60 mM KCl, 5% Glycerol, 1.5 mM DTT, 2mM $MgCl_2$) for 3 hours in 4°C. Buffer B and buffer C (Buffer B: 20 mM HEPES-KOH pH 7.55, 60 mM KCl, 10% Glycerol, 1 mM DTT, 2 mM $MgCl_2$ / Buffer C: 20 mM HEPES pH 7.55, 60 mM KCl, 30% Glycerol, 1 mM DTT, 2 mM $MgCl_2$, 0.1% Glutaraldehyde) were mixed using gradient maker (Gradient Master, Biocomp). Prepared sample was then added on the top layer of the tube mixture and centrifuged overnight (Beckman Coulter Optima XL-100K). Solution in the tube was then fractionated and analyzed.

Electron microscopy sample preparation and data collection

Continuous carbon grids were glow-discharged for 30 seconds using Pelco easiGlow Cleaning System. We then deposited 3 microliters of purified sample, incubated it for 30 seconds on the grid at room temperature, negatively stained with 5 drops of 2% uranyl formate solution and blotted dry. The grids were imaged using a Tecnai G^2 20 X-TWIN electron microscope equipped with a LaB6 source, operating at 200 keV at a nominal magnification of 17,500× (6.07 Å/pixel at the detector level).

The images were recorded on Gatan US1000XP Ultrascan CCD camera (2048 x 2048, 14 μm physical pixel size, Figure S17), at a defocus range of −1.5 to −3 μm, and an electron dose of 25 $e^-/Å^2$.

Image processing

The collected images were contrast-inverted using EMAN2(23) and imported into cryoSPARC v2.15(24) for all subsequent data processing. After CTF calculations, 1500 particles were picked

manually, classified in 2D and used as templates for automated particle picking. After picking, 2D classification was used to eliminate "bad particles", and the selection was used for Ab initio and subsequently Homogeneous refinement. We also used 3D classification to further homogenize the sample in silico.

Heme incorporation of DcpG WT

The heme incorporation was calculated using the pyridine hemachromagen assay to determine the concentration of the heme.(25) The concentration of DcpG heme was 25 μM and the protein concentration, determined by Bradford assay was 30.6 μM. Therefore, the heme incorporation ((heme concentration / protein concentration)*100) of DcpG was calculated to be to be 81.7%.

Heme autooxidation

Purified DcpG in the Fe(II)-O_2 state was used for the autooxidation experiment. Following reduction of the heme and O_2 binding to form the Fe(II)-O_2 complex, the absorbance changes of the Soret and the UV-vis α/β region for 10 μM of DcpG were monitored using an Agilent Cary 100 spectrophotometer using scanning kinetics.

Equilibration of DcpG Fe(III) in phosphate buffer

To chemically oxidize DcpG, the protein was brought into the anaerobic chamber as DcpG Fe(II)-O_2 and buffer exchanged in to 100 mM KH_2PO_4 50 mM KCl pH 7.0, 100 mM Hepes 50 mM KCl pH 7.0, 50 mM Hepes 50 mM KCl pH 7.0 or 50 mM Hepes 50 mM KCl pH 7.5 (oxidation of DcpG in Tris buffer leads to either conformational changes that allow binding of a side chain to the heme or binding of a Tris molecule to the heme). After buffer exchange into the appropriate buffer DcpG Fe(II)-O_2 was oxidized using ~10-equivalents of potassium ferricyanide. The protein was then transferred to a sealed cuvette, removed from the anerobic chamber, and changes in DcpG Fe^{III} ligation and/or spin state monitored using UV-visible absorbance for 1 hr or 24 hrs.

Electrochemical oxidation was performed by reducing with sodium dithionite, followed by buffer exchanging into 50mM HEPES, 50 mM NaCl pH 7.5, and transferring into a spectro-electrochemistry cuvette, to which 45 μL of redox mediators (see below) were added. After sealing the cell, it was removed from the anaerobic chamber, purged with argon, and an oxidizing potential (500 mV vs SHE) was applied for ~14 hrs.

Circular dichroism (CD) spectroscopy

CD measurements were performed on a JASCO J-1500 spectrometer, equipped with a Peltier model PTC-517 thermostatted cell holder. Signals were recorded from 260 nm to 180 nm with a scan speed of 50 nm min^{-1} and a band width of 1 nm at 20 ºC. The quartz cell used was 1 mm. The proteins were prepped as previously described and the final protein concentrations were 0.1 mg/ml.

Dynamic Light Scattering

DcpG samples were checked for their quality and mono-dispersity with a dynamic light scattering (DLS) run prior to the small angle x-ray scattering experiment. All proteins were in the Fe(II)-O_2 ligation state. DLS experiments of DcpG Fe(II)-O_2 (0.5 mg/mL) were performed using a Viscotec 802 instrument at 293 K. The DLS data were processed by the OmniSIZE 3.0 software to get an estimate for the hydrodynamic radius (R_h) and polydispersity of the protein sample. The estimated R_h for DcpG, DcpG H62W DcpG R79Q, DcpG H62A was 5.19, 4.39, 5.92, 5,75 nm,

respectively. The estimated R_h suggested a monodisperse distribution of a dimer of DcpG and its variants existed in solution (**Figure S13 and Table S1**).

DcpG cross-linking experiment and analysis

DcpG Fe(II), Fe(II)-O_2, Fe(II)-CO, Fe(II)-NO ligation states were prepared as previously described in Patterson et al. A BS^3 crosslinker (12.5 mM, Thermo Scientific) stock solution was prepared in 20mM sodium phosphate buffer pH 7.5 (anaerobic buffer for Fe(II), Fe(II)-NO, and Fe(II)-CO reactions and aerobic buffer for Fe(II)-O_2 reaction). The crosslinking reaction consisted of a final concentration of 15 µM DcpG in the respective ligation state, 10 mM $MgCl_2$, and varying BS^3 crosslinker concentration (15 µM, 150 µM, 375 µM, and 750 µM). The reaction incubated at room temperature for 30 min. then quenched by adding 10 µL of Tris buffer H 7.5 to a final concentration of 20 mM.

To determine if the crosslinking reaction worked, 10 µL of each crosslinking reaction was ran on an SDS gel with un-crosslinked DcpG as a comparison (supporting figure). The rest of the reaction was flash frozen then sent to The Pennsylvania State University Hershey College of Medicine Mass Spec and Proteomics Core for analysis. The samples were precipitated in 80% Acetone/Water and store at -20°C over night. Samples were then reduced with tris(2-carboxyethyl)phosphine (TCEP), alkylated with iodoacetamide, then digested with Trypsin/LysC overnight at 37 C. The samples were dried, cleaned on a C18 cartridge and dried. The equivalent of 2ug from a sample was auto-injected using a Eksigent NanoLC-Ultra-2D Plus and Eksigent 200 µm x 0.5 mm C18-CL 3 µm 120 Å trap Column and eluted through a Eksigent 3 C18 CL, 75um 15cm Nano Column. The buffers used were for the elution were 0.1% folic acid in H_2O (Buffer D) and 0.1% folic acid in acetonitrile (Buffer E). The parameters for the elution gradient were 95% Buffer D / 5% Buffer E (300nl per minute flowrate) to 65% Buffer D / 35% Buffer E in 60 minutes, 15% Buffer D / 85% Buffer E from 60 to 70 minutes, then 95% Buffer D / 5% Buffer E from 70-90 min. Calibration runs were done in between each sample.

The ABSciex 5600 TripleTOF settings used: Parent scan acquired for 250 msec, then up to 50 MS/MS spectra acquired over 2.5 seconds for a total cycle time of 2.8 seconds. Gas 1(Nitrogen)= 2 Gas 3(Nitrogen)= 25.

The wiff files produced were analyzed using Protein Pilot 5. The database used was DcpG sequence provided by the lab concatenated to a 536 common contaminant lab database. All mgf files collected were then used by Plink software to obtain the crosslink data using BS3-d_0 crosslinker.

Crosslinks were identified between peptides of DcpG in the Fe(II), Fe(II)-O_2, and Fe(II)-NO ligation states; DcpG Fe(II)-CO samples did not yield any identifiable crosslinks. Crosslinks between the sensor globin and DGC domains were identified for DcpG Fe(II) and Fe(II)-NO, but were not observed for Fe(II)-O_2 samples (**Figure S15**, **Table S5**).

Supplemental Figures

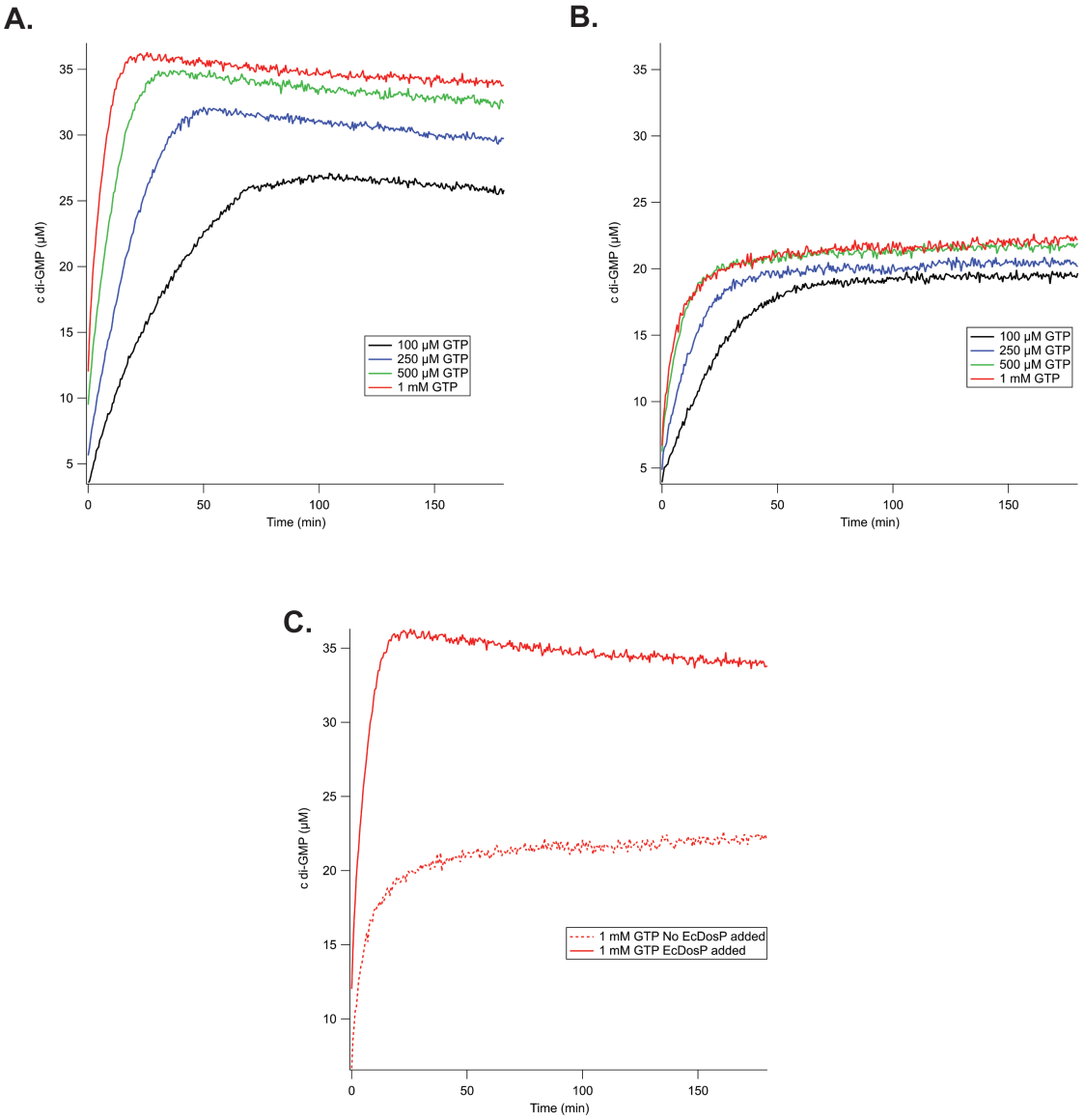

Figure S1. DcpG diguanylate cyclase domain exhibits product inhibition. (A) Rate plots for 1.7 µM DcpG Fe(II) with 3-fold molar excess of *Ec*DosP at various GTP concentrations (B) Rate plots for 1.7 µM DcpG Fe(II) without *Ec*DosP at various GTP concentrations (C) Direct comparison for 1mM GTP.

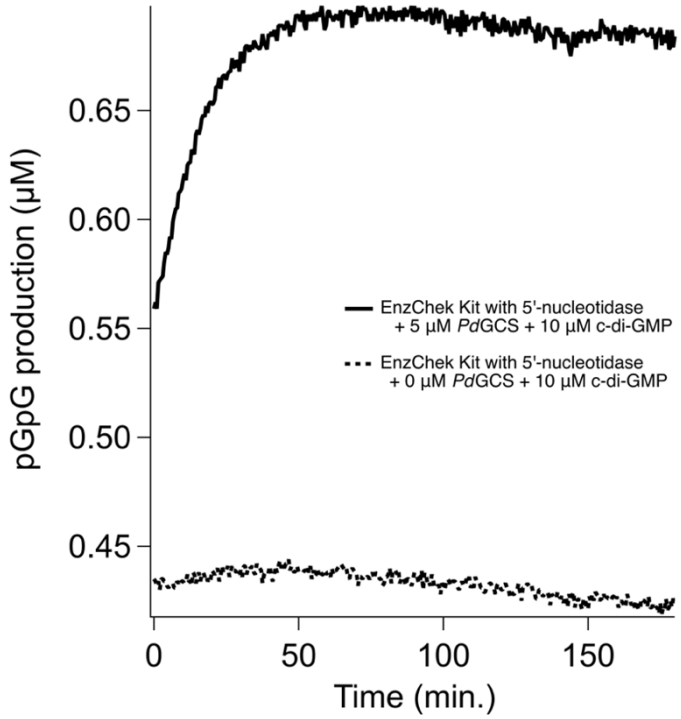

Figure S2. EnzChek 5'-nucleotidase control for PDE assay demonstrates that c-di-GMP is not a substrate of the 5'-nucletotidase enzyme. The 5'-nucleotidase only reacts with the product of c-di-GMP hydrolysis, pGpG.

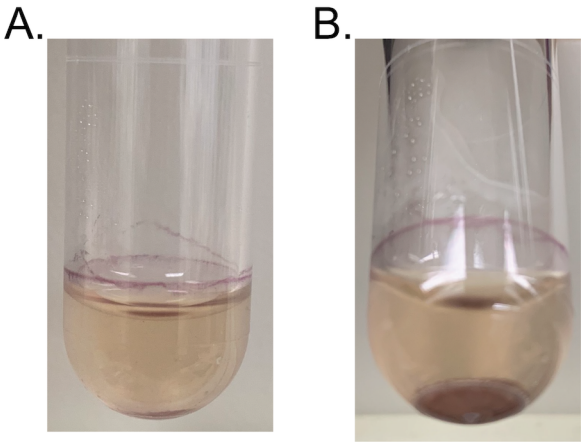

Figure S3. Congo Red staining of *P. dendritiformis* biofilm formation from the side (A.) and tilted (B.).

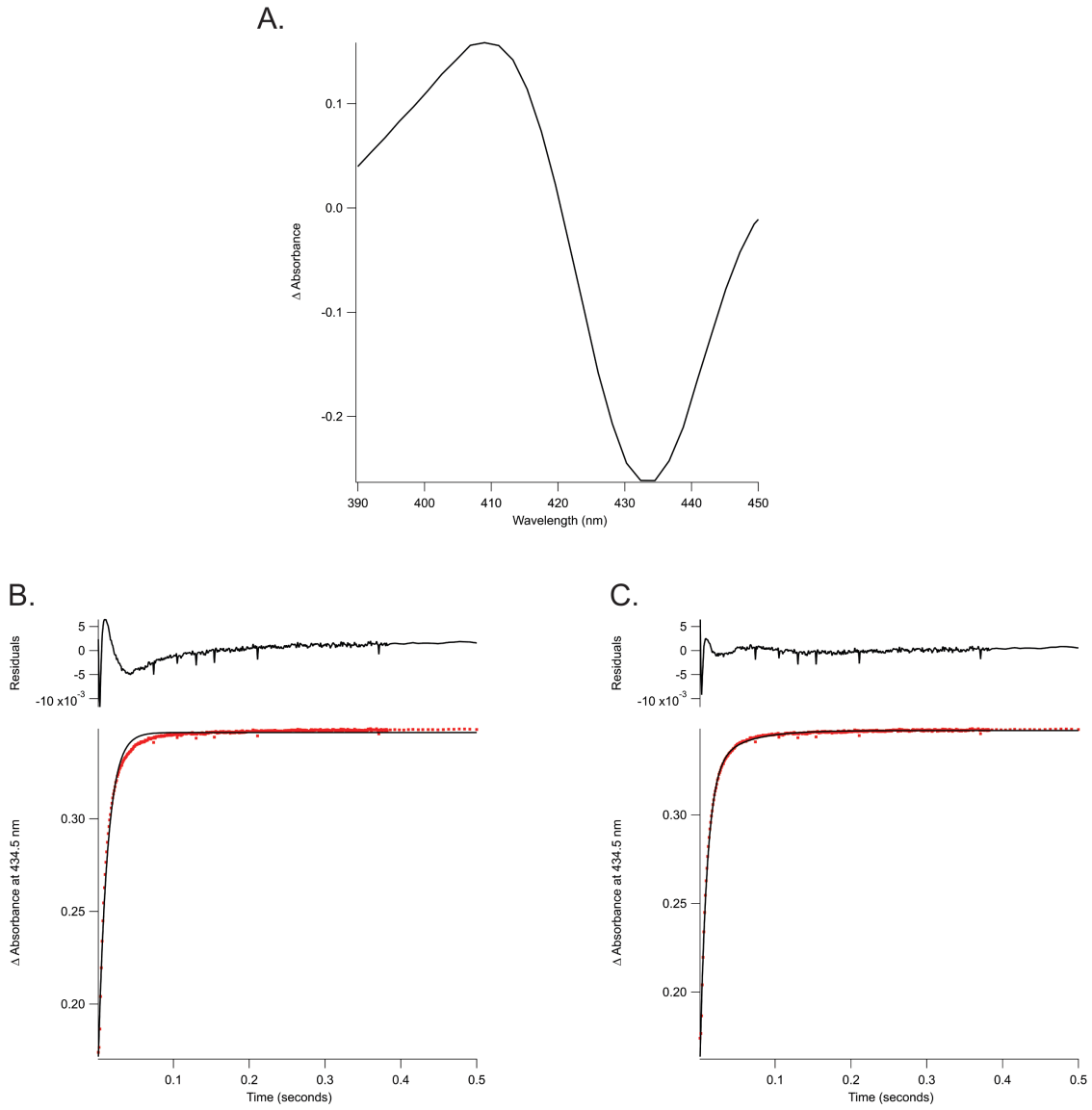

Figure S4. Stopped-flow kinetics fitting of DcpG O_2 dissociation rates. (A) Difference spectra to determine maximum and minimum wavelengths. Comparison of mono-exponential and bi-exponential fits for DcpG and variants experiments (B. and C., respectively) The fit residuals (difference between calculated fit (red line) and raw data (black line)) are shown in red above each graph.

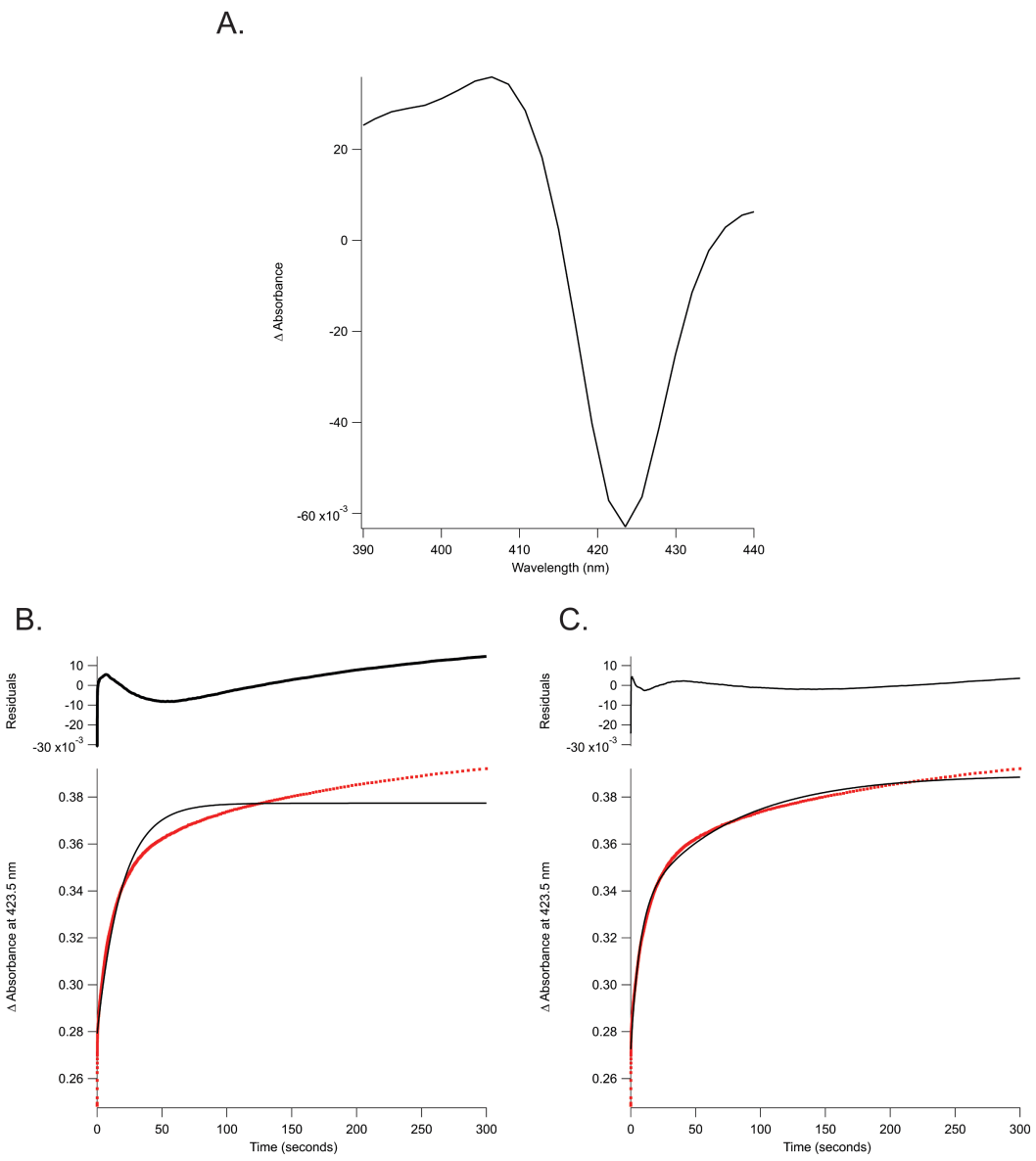

Figure S5. Stopped-flow kinetics fitting of DcpG NO dissociation rates. A) Difference spectra to determine maximum and minimum wavelengths. Comparison of mono-exponential and bi-exponential fits for DcpG and variants experiments (A. and B., respectively) The fit residuals (difference between calculated fit (red line) and raw data (black line)) are shown in red above each graph.

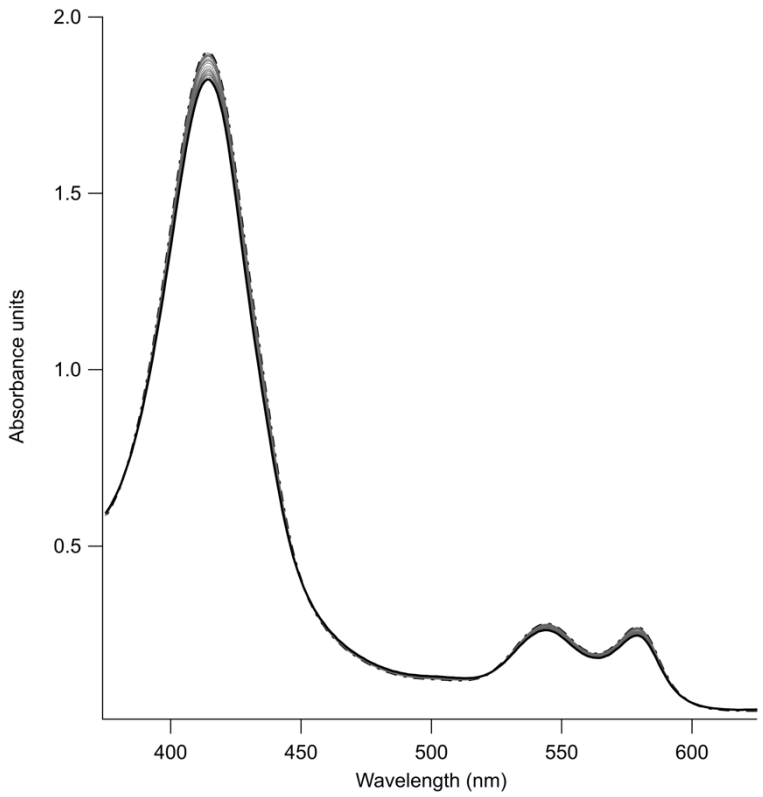

Figure S6. DcpG does not exhibit measurable auto-oxidation. Scanning kinetics of DcpG Fe(II)-O_2 over a 20-hour period at room temperature demonstrating that there is no shift in absorbance maxima of the Soret or a/b bands of the heme spectrum.

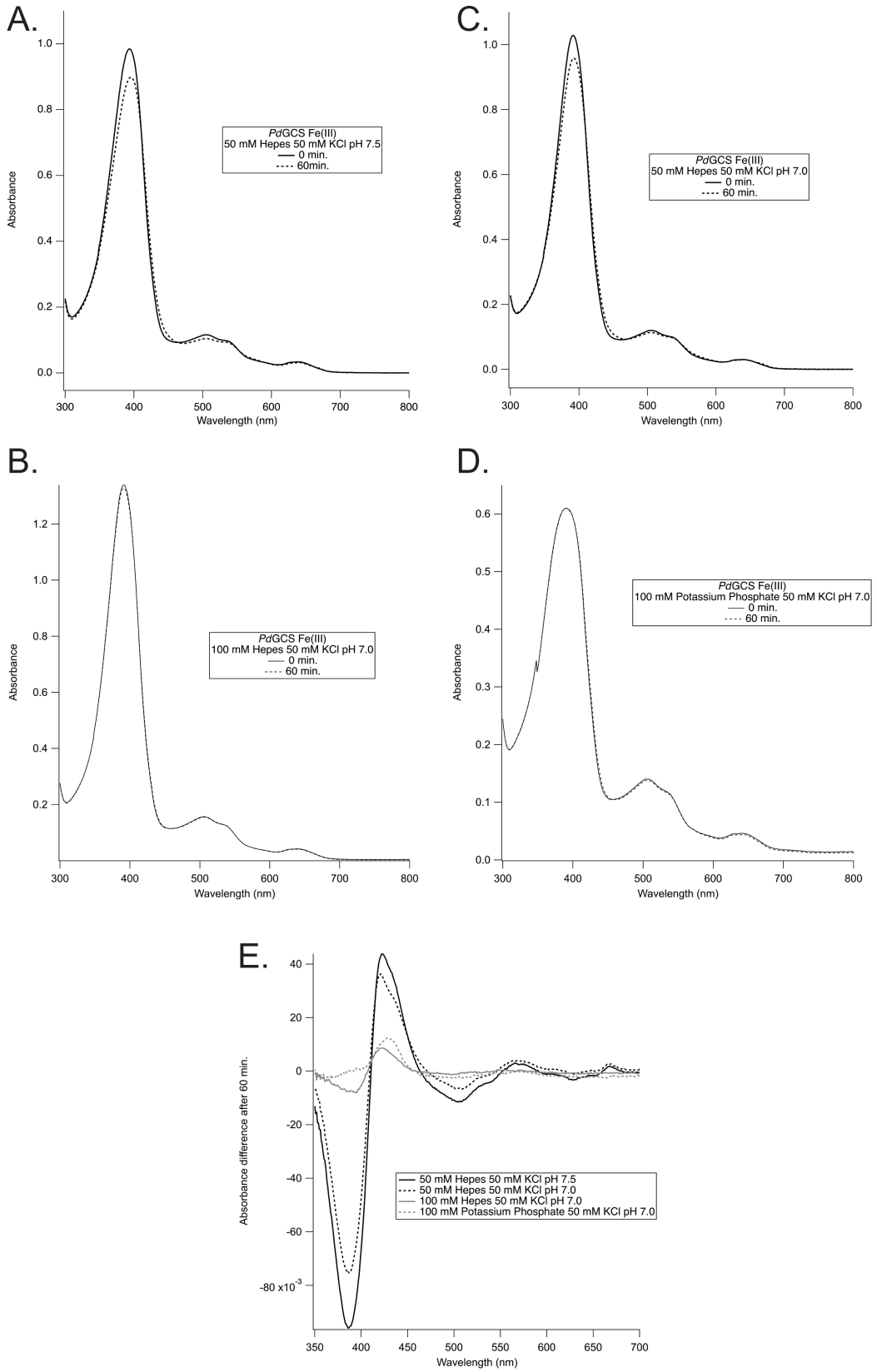

Figure S7. DcpG Fe(III) equilibration in HEPES and phosphate buffers. (A) DcpG Fe(III) in 50 mM hepes 50 mM KCl pH 7.5 shows gradual shift in Soret and α/β bands in 60 min. (B) DcpG

Fe(III) in 100 mM hepes 50 mM KCl pH 7.0 shows minimal shift in Soret and α/β bands in 60 min (C) DcpG Fe(III) in 50 mM hepes 50 mM KCl pH 7.0 shows gradual shift, but less than pH 7.5, in Soret and α/β bands in 60 min. (D) DcpG Fe(III) in 100 mM potassium phosphate 50 mM KCl pH 7.0 shows minimal shift in Soret and α/β bands in 60 min. (D) Difference spectra between DcpG Fe(III) in phosphate and hepes buffer after 60 min.

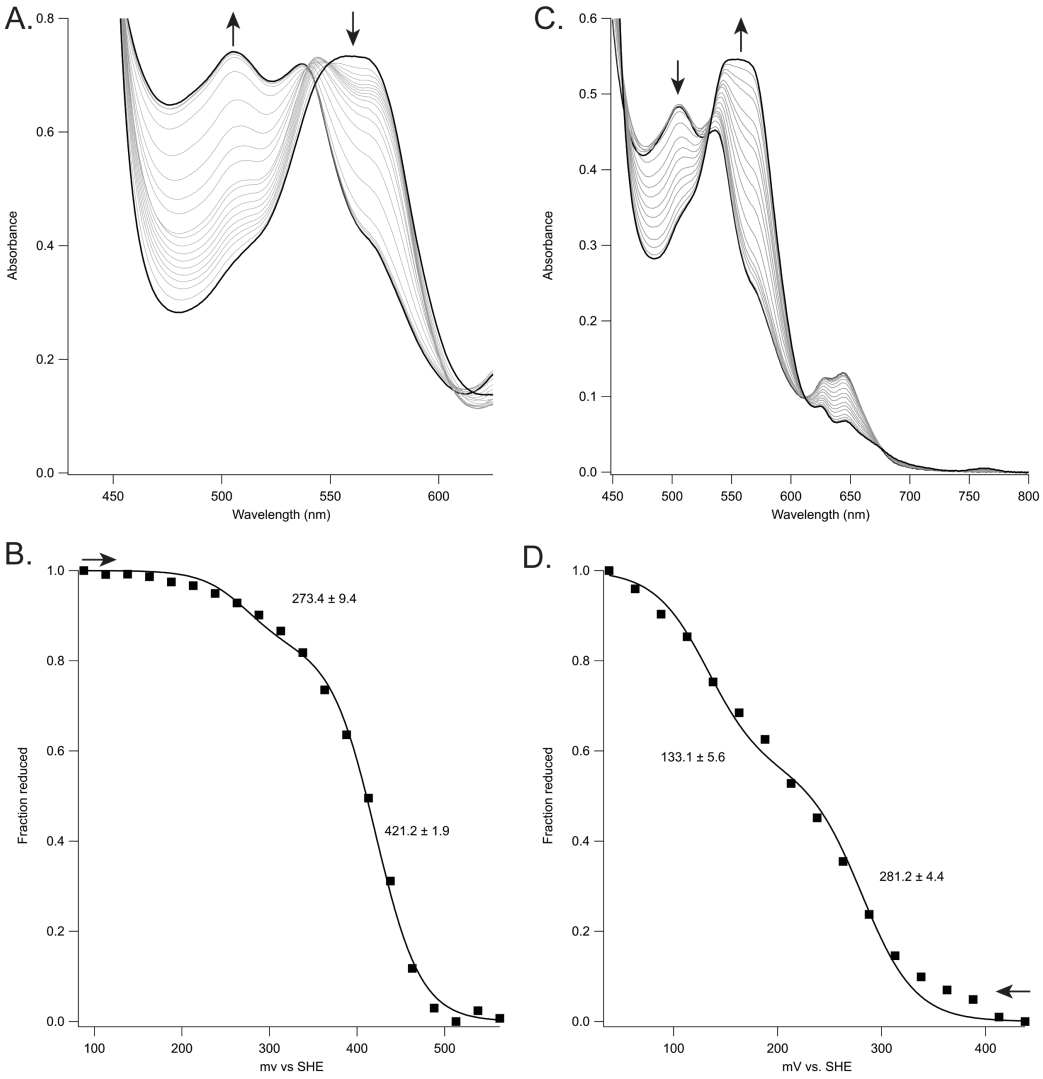

Figure S8. DcpG reductive and oxidative titration in 50 mM Hepes 50 mM KCl pH 7.5. A. and B.) Spectral changes and Nernst fit of a representative reductive titration. C. and D.) Spectral changes and Nernst fit of a representative oxidative titration.

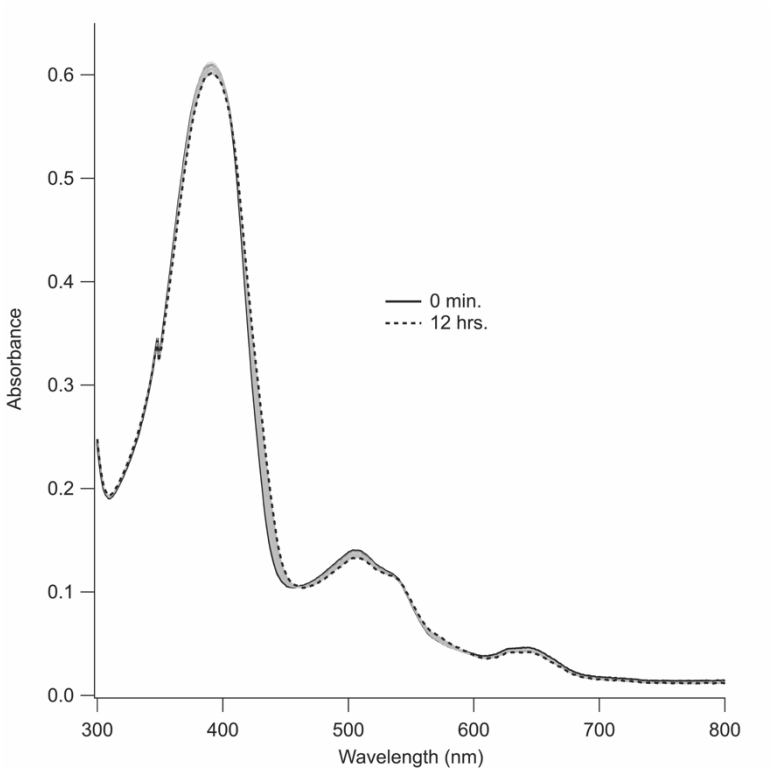

Figure S9. Equilibration of DcpG Fe(III) in 100 mM potassium phosphate 50 mM KCl pH 7.0 over 12 hrs.

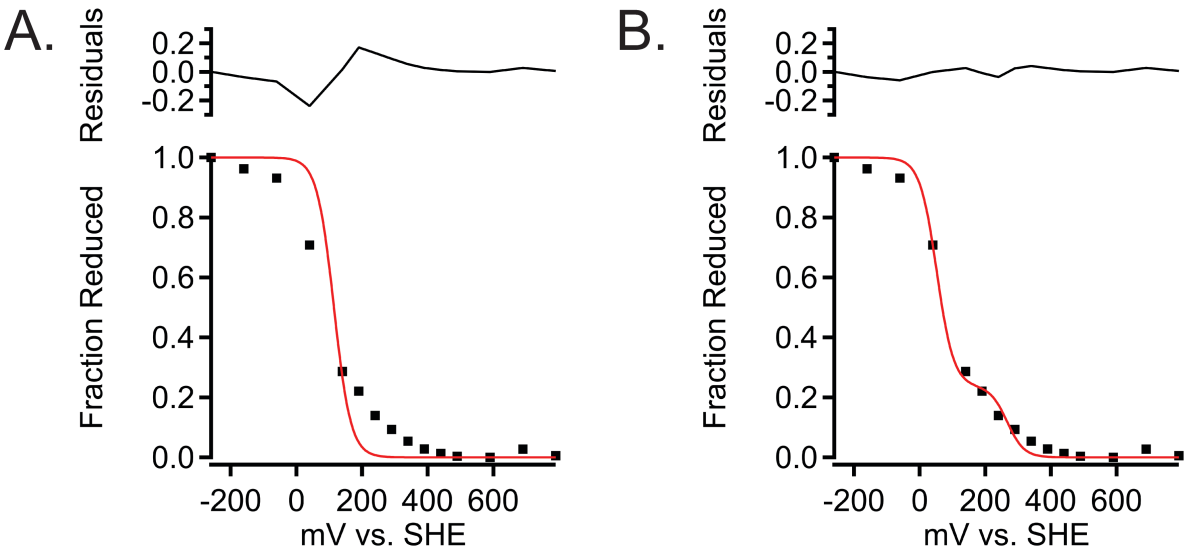

Figure S10. (A) Single and (B) double midpoint fit comparison for DcpG reductive titration in 100 mM potassium phosphate 50 mM KCl pH 7.0. The residuals are plotted above the graph (A) and (B) graphs to display the best fit.

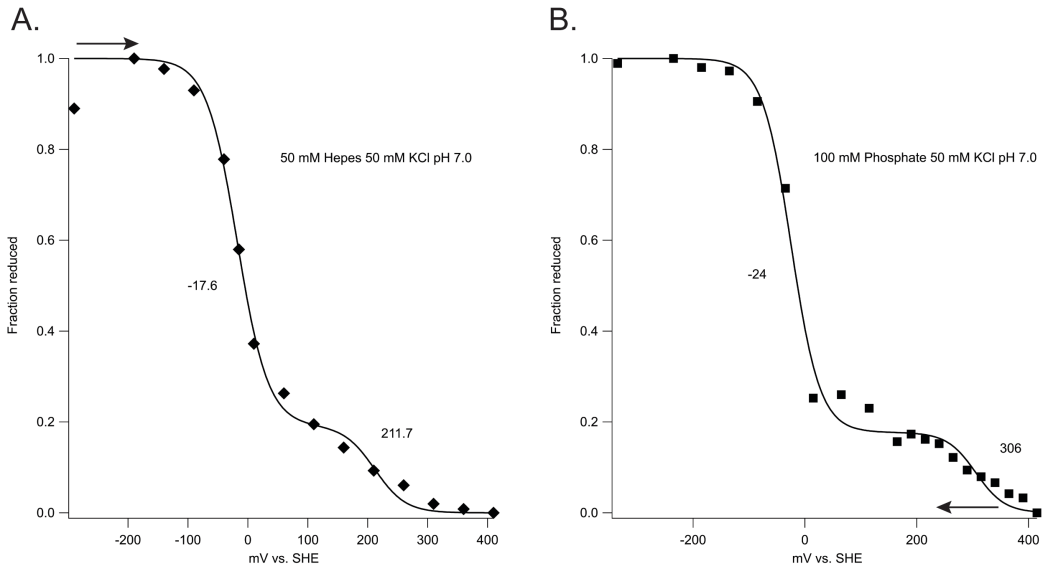

Figure S11. Representative reductive (A.) and oxidative (B.) titrations of *Pcc*GCS.

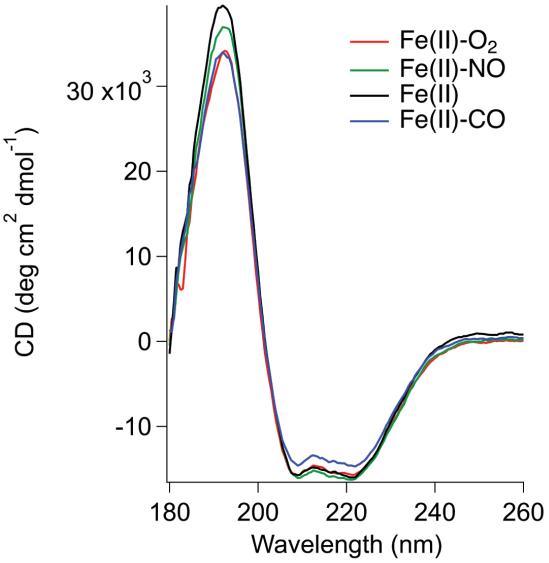

Figure S12. CD spectra wild-type DcpG in various ligation states.

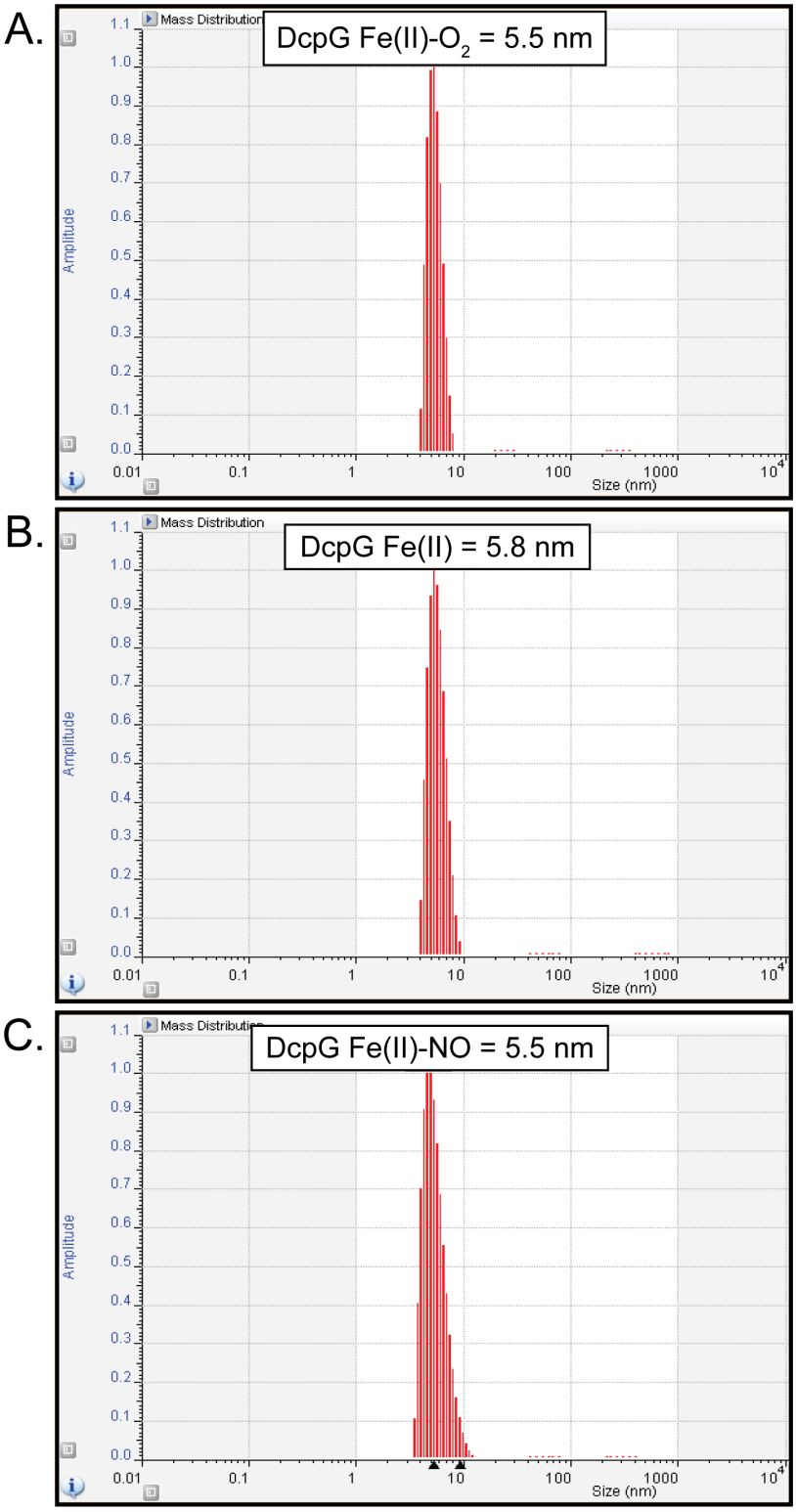

Figure S13. Dynamic Light Scattering of DcpG in (A) Fe(II)-O_2, (B) Fe(II), and (C) Fe(II)-NO ligation states. The hydrodynamic diameter is listed on each graph.

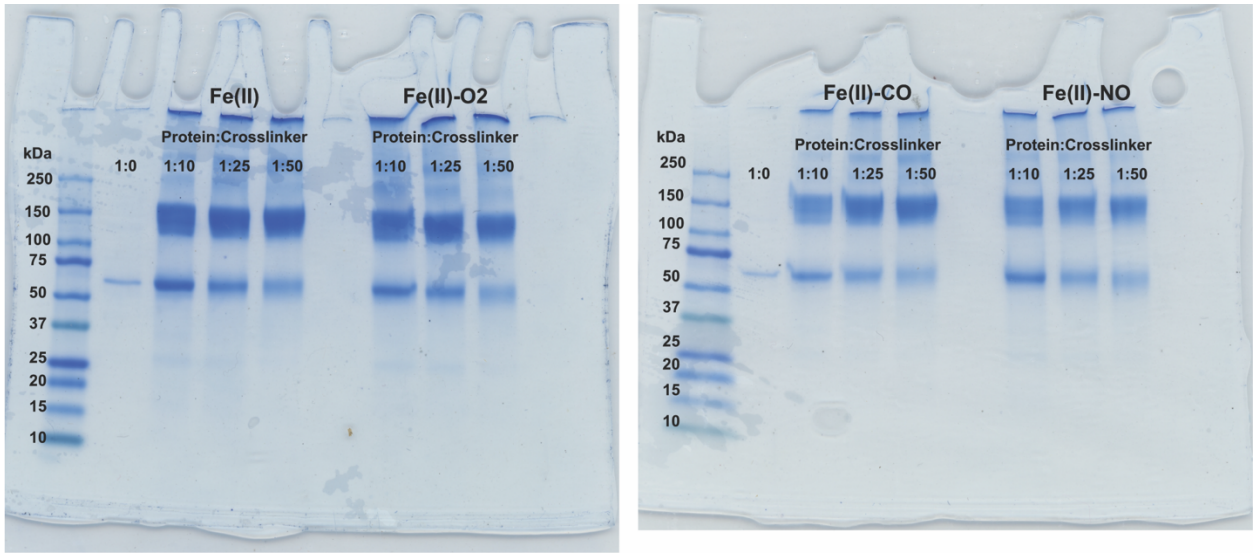

Figure S14. SDS gels of DcpG crosslinking reactions for each ligation state. The ratio of protein:crosslinker concentration is labeled on the gels.

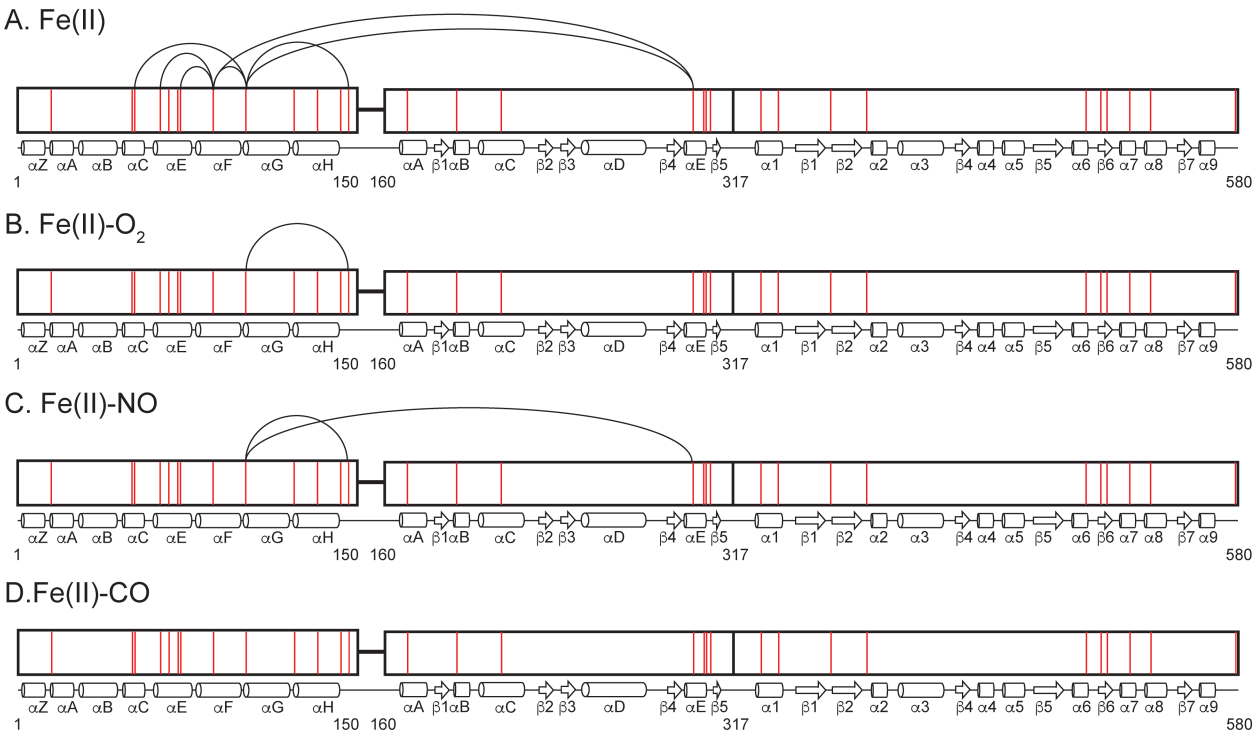

Figure S15. Visual representation of DcpG crosslinking results with BS3-d0 for A.) DcpG Fe(II); B.) DcpG Fe(II)-O_2, C.) DcpG Fe(II)-NO, and D.) DcpG Fe(II)-CO. Results were generated by pLink2.(26)

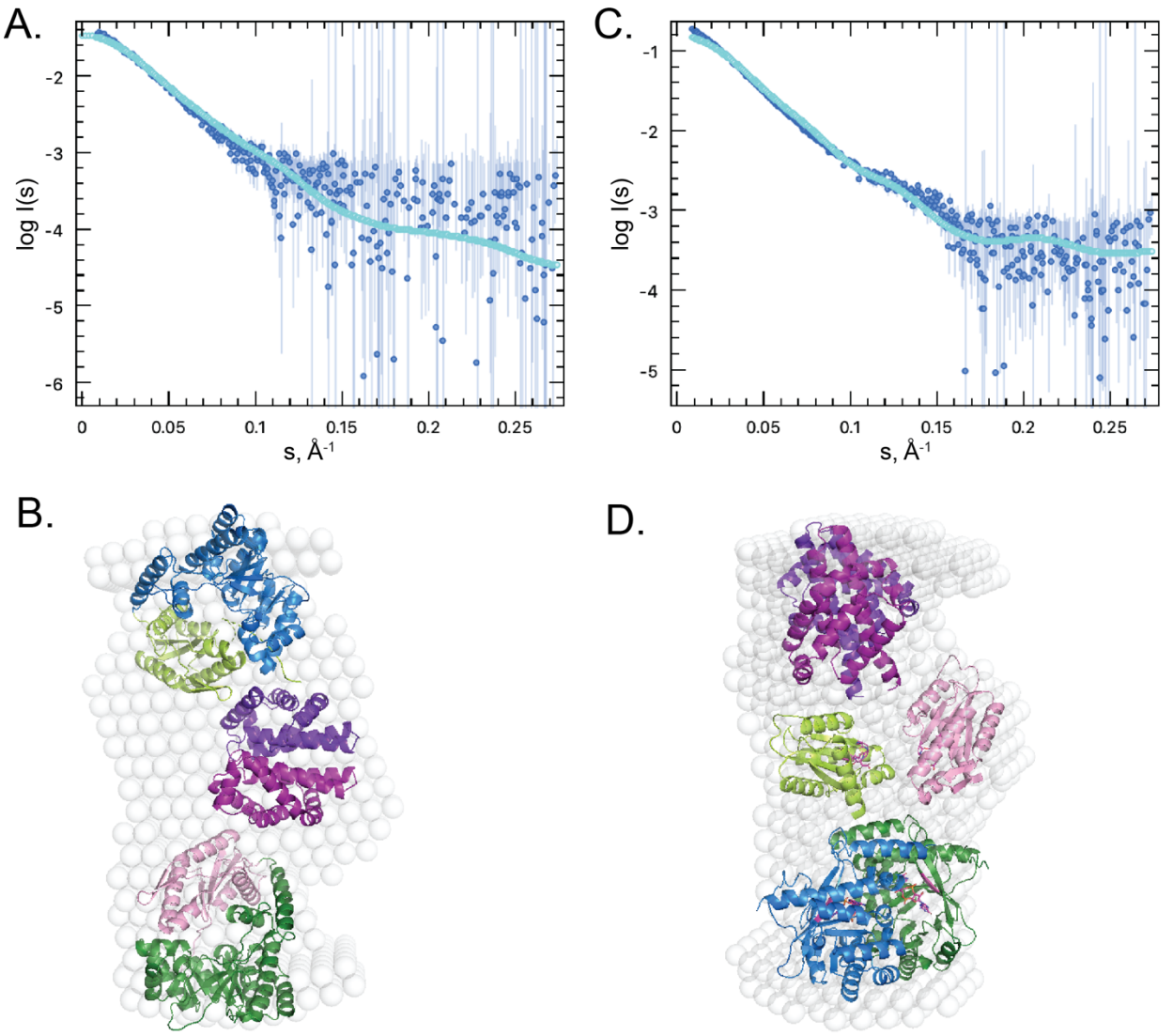

Figure S16. ATSAS-Crysol program overlay of calculated SAXS profiles from models for the pseudo-symmetric (A., B.) and extended (C., D.) DcpG dimer models (aqua lines) with experimental data (blue dots).

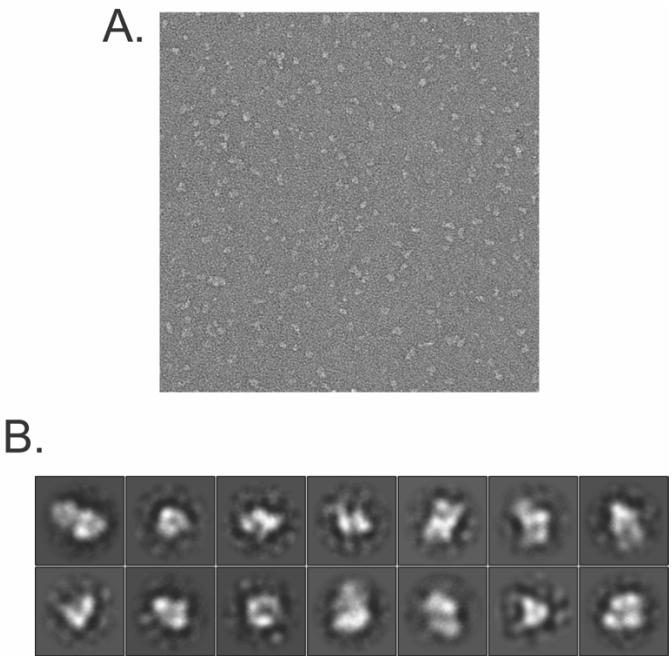

Figure S17. (A) Representative negative stain EM image of DcpG. (B) 2D class averages of DcpG

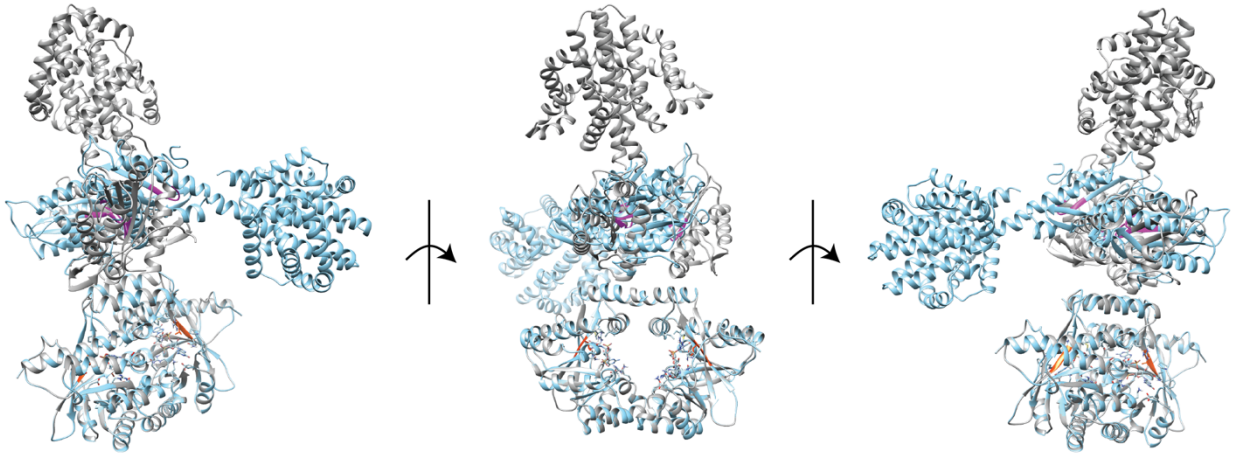

Figure S18. Overlays of DcpG models derived from SAXS (gray) and negative stain EM (blue). The EAL domains overlay and maintain the dimeric active site (residues highlighted in orange). While a rotation is observed within the GGDEF domains, the active sites (magenta) are distant from each other, yielding low enzymatic activity. The largest difference is observed in the globin domains, which are bent in the negative stain EM model, relative to the SAXS model. The differences in the data obtained from the two techniques supports the flexibility of the linkers in DcpG and the ability of the protein to exist in different conformational states.

Supplemental Tables

Table S1. DLS results for DcpG

WT DcpG						
Peak	% Area	Rh (nm)	Position	% RSD	MW (kD)	Unres. Peaks
1	100	5.19	4.68	20	161.71	10.00 nm; 5.01 nm

Table S2. DcpG O_2 dissociation rates are independent of sodium dithionite concentration

Rates from ProK	5 mM $Na_2S_2O_4$	10 mM $Na_2S_2O_4$	15 mM $Na_2S_2O_4$	30 mM $Na_2S_2O_4$
k_1	11.44	12.01	12.27	11.08
k_2	83.30	87.30	88.35	86.23

Table S3. DcpG O_2 dissociation rates are independent of sodium dithionite concentration and CO

Rates from ProK	5 mM $Na_2S_2O_4$ + CO	50 mM $Na_2S_2O_4$ + CO	50 mM $Na_2S_2O_4$
k_1	0.15	0.15	0.12
k_2	0.014	0.012	0.012

Table S4. CD Analysis of DcpG WT

Ligation State	**Helix**	**Antiparallel**	**Parallel**	**Turn**	**Others**
Fe(II)	38.3	17.6	0.0	4.5	39.6
Fe(II)-O_2	37.6	6.5	8.5	9.4	38.1
Fe(II)-NO	37.8	8.6	6.9	7.9	39.0
Fe(II)-CO	34.8	18.6	1.0	5.6	38.7

Table S5. Cross-linked peptides for DcpG in different ligation states. Numbering includes His-tag (+10 from untagged numbering).

Peptides	Peptide1 Range	Peptide2 Range	X-link 1	X-link 2
DcpG Fe(II)				
IDPEFIEKR(8)-IGLKTR(4)	81-89	99-104	88	102
KHLIEMFSGR(1)-IDPEFIEKR(8)	71-80	81-89	71	88
KLILEHSQIEK(1)-IGLKTR(4)	54-64	99-104	54	102
LILEHSQIEKLR(10)-IDPEFIEKR(8)	55-66	81-89	64	88
NADKAMYEVK(4)-IDPEFIEKR(8)	307-316	81-89	310	88
NADKAMYEVK(4)-IGLKTR(4)	307-316	99-104	310	102
RSNEKIQHQAFHDELTGLPNRR(5)-IGLKTR(4)	156-177	99-104	160	102
SNEKIQHQAFHDELTGLPNR(4)-IGLKTR(4)	157-176	99-104	160	102
SNEKIQHQAFHDELTGLPNRR(4)-IGLKTR(4)	157-177	99-104	160	102
DcpG Fe(II)-O_2				
SNEKIQHQAFHDELTGLPNR(4)-IGLKTR(4)	157-176	99-104	160	102
DcpG Fe(II)-NO				
99-104	310	102		
99-104	160	102		

Table S6. SAXS structural parameters of DcpG

Guinier analysis	**DcpG WT**
$I(0)$ (cm^{-1})	0.1953
R_g (Å)	59.5
q min (Å $^{-1}$)	0.0096
q max (Å $^{-1}$)	0.0198
***P(r)* analysis**	
$I(0)$ (cm^{-1})	0.1910
R_g (Å)	59.15
D_{max} (Å)	205.0
q range (Å $^{-1}$)	0.0096- 0.2746

Porod volume (Å^3)	204662

Equation S1. Nernst equation for two midpoint potentials in mV

$$f(x) = \left(c \times \frac{\left(e^{(-0.038921 \times (x-a))}\right)}{1 + \left(e^{(-0.038921 \times (x-a))}\right)}\right) + \left((1-c) \times \frac{\left(e^{(-0.038921 \times (x-b))}\right)}{1 + \left(e^{(-0.038921 \times (x-b))}\right)}\right)$$

a = midpoint 1
b = midpoint 2
c = fraction of midpoint 1

REFERENCES

1. C. Suter-Crazzolara, K. Unsicker, Improved expression of toxic proteins in E.coli. *BioTechniques*, 202-204 (1995).
2. E. M. Boon, S. H. Huang, M. A. Marletta, A molecular basis for NO selectivity in soluble guanylate cyclase. *Nature Chem Biol* **1**, 53-59 (2005).
3. D. S. Karow *et al.*, Spectroscopic Characterization of the Soluble Guanylate Cyclase-like Heme Domains from Vibrio cholerae and Thermoanaerobacter tengcongensis. *Biochemistry* **43**, 10203-10211 (2004).
4. Y. Ishitsuka *et al.*, Arg97 at the heme-distal side of the isolated heme-bound PAS domain of a heme-based oxygen sensor from Escherichia coli (Ec DOS) plays critical roles in autoxidation and binding to gases, particularly O2. *Biochemistry* **47**, 8874-8884 (2008).
5. J. L. Burns, D. D. Deer, E. E. Weinert, Oligomeric state affects oxygen dissociation and diguanylate cyclase activity of globin coupled sensors. *Mol Biosyst* **10**, 2823-2826 (2014).
6. J. L. Burns *et al.*, Oxygen and c-di-GMP Binding Control Oligomerization State Equilibria of Diguanylate Cyclase-Containing Globin Coupled Sensors. *Biochemistry* **55**, 6642-6651 (2016).
7. R. Paul *et al.*, Cell cycle-dependent dynamic localization of a bacterial response regulator with a novel di-guanylate cyclase output domain. *Genes & Development* **18**, 715-727 (2004).
8. X. Wan *et al.*, Globins synthesize the second messenger bis-(3'-5')-cyclic diguanosine monophosphate in bacteria. *J Mol Biol* **388**, 262-270 (2009).
9. A. J. Spiers, J. Bohannon, S. M. Gehrig, P. B. Rainey, Biofilm formation at the air-liquid interface by the Pseudomonas fluorescens SBW25 wrinkly spreader requires an acetylated form of cellulose. *Mol. Microbiol.* **50**, 15-27 (2003).
10. E. E. Weinert, L. Plate, C. A. Whited, C. Olea, Jr., M. A. Marletta, Determinants of ligand affinity and heme reactivity in H-NOX domains. *Angew Chem* **49**, 720-723 (2010).
11. J. M. Brisendine, A. C. Mutter, J. F. Cerda, R. L. Koder, A three-dimensional printed cell for rapid, low-volume spectroelectrochemistry. *Anal Biochem* **439**, 1-3 (2013).

12. J. B. Hopkins, R. E. Gillilan, S. Skou, BioXTAS RAW: improvements to a free open-source program for small-angle X-ray scattering data reduction and analysis. *Journal of Applied Crystallography* **50**, 1545-1553 (2017).
13. D. Franke *et al.*, ATSAS 2.8: a comprehensive data analysis suite for small-angle scattering from macromolecular solutions. *Journal of Applied Crystallography* **50**, 1212-1225 (2017).
14. D. I. Svergun, Determination of the regularization parameter in indirect-transform methods using perceptual criteria. *Journal of Applied Crystallography* **25**, 495-503 (1992).
15. D. I. Svergun, Restoring Low Resolution Structure of Biological Macromolecules from Solution Scattering Using Simulated Annealing. *Biophysical Journal* **76**, 2879-2886 (1999).
16. V. V. Volkov, D. I. Svergun, Uniqueness of ab initio shape determination in small-angle scattering. *Journal of Applied Crystallography* **36**, 860-864 (2003).
17. D. Svergun, C. Barberato, M. H. J. Koch, CRYSOL – a Program to Evaluate X-ray Solution Scattering of Biological Macromolecules from Atomic Coordinates. *Journal of Applied Crystallography* **28**, 768-773 (1995).
18. J. Yang *et al.*, The I-TASSER Suite: protein structure and function prediction. *Nature Methods* **12**, 7-8 (2015).
19. Anonymous (The PyMOL Molecular Graphics System, Version 1.2r3pre, Schrödinger, LLC.
20. E. F. Pettersen *et al.*, UCSF Chimera--A visualization system for exploratory research and analysis. *Journal of Computational Chemistry* **25**, 1605-1612 (2004).
21. A. Panjkovich, D. I. Svergun, Deciphering conformational transitions of proteins by small angle X-ray scattering and normal mode analysis. *Physical Chemistry Chemical Physics* **18**, 5707-5719 (2016).
22. B. Kastner *et al.*, GraFix: sample preparation for single-particle electron cryomicroscopy. *Nature Methods* **5**, 53-55 (2008).
23. G. Tang *et al.*, EMAN2: An extensible image processing suite for electron microscopy. *Journal of Structural Biology* **157**, 38-46 (2007).
24. A. Punjani, J. L. Rubinstein, D. J. Fleet, M. A. Brubaker, cryoSPARC: algorithms for rapid unsupervised cryo-EM structure determination. *Nature Methods* **14**, 290-296 (2017).
25. I. Barr, F. Guo, Pyridine Hemochromagen Assay for Determining the Concentration of Heme in Purified Protein Solutions. *Bio-protocol* **5** (2015).
26. Z.-L. Chen *et al.*, A high-speed search engine pLink 2 with systematic evaluation for proteome-scale identification of cross-linked peptides. *Nature Communications* **10**, 3404 (2019).